Spatio-temporal analysis of vascular endothelial growth factor expression and blood vessel remodelling in pig ovarian follicles during the periovulatory period

A Martelli, P Berardinelli, V Russo, A Mauro, N Bernabò, L Gioia, M Mattioli and **B Barboni**

Department of Comparative Biomedical Sciences, University of Teramo, Piazza A. Moro, 45, 64100 Teramo, Italy

(Requests for offprints should be addressed to A Martelli; Email: amartelli@unite.it)

Abstract

Vascular endothelial growth factor (VEGF) expression pattern and blood vessel remodelling were evaluated during the transition from the preovulatory follicle to the corpus luteum (CL). To this end, prepubertal gilts were treated with equine chorionic gonadotrophin (eCG) to collect preovulatory follicles (60 h after eCG) and with human chorionic gonadotrophin (hCG) to obtain periovulatory follicles 18 h and 36 h later. The VEGF mRNA content was analysed by *in situ* hybridization, while protein localization in follicular fluid (FF) and in granulosa and theca compartments was evaluated by ELISA, immunohistochemistry or western blot. Blood vessel architecture and vascular area (VA) were investigated using immunohistochemistry for von Willenbrand Factor, a specific endothelial marker. Vascular remodelling was finally tested using Ki-67 immunocytochemistry as a proliferation marker, or α-smooth muscle actin (α-SMA) as a specific mural cell marker. eCG-treated follicles showed high VEGF levels and two concentric blood vessel networks composed of proliferating endothelial cells without any association with mural components. hCG injection inhibited VEGF synthesis in the granulosa compartment and, as a consequence, the protein fell within the FF. In parallel, endothelial cell proliferation stopped and the VA decreased. Close to ovulation, VEGF production restarted in both follicular compartments and VEGF mRNA content significantly increased in the theca layer. Changes in follicular VEGF secretion were observed; the protein disappeared from FF and was observed in the extracellular matrix. An active angiogenesis characterized the follicle; endothelial cell proliferation was associated with a recruitment of α-SMA-positive mural cells. The data presented in this work showed that, in the phases preceding ovulation, a complete vascular remodelling occurs, characterized by both an evident neovascularization and the appearance of blood vessels presenting smooth musculature which could be involved in CL formation after ovulation.

Journal of Molecular Endocrinology (2006) **36,** 107–119

Introduction

Ovarian vasculature size and morphology undergo marked changes throughout the oestrous cycle (Bjersing & Cajander 1974, Redmer & Reynolds 1996, Jiang *et al.* 2003). It has been reported that the regulation of ovarian angiogenesis is markedly dependent on the secretion of vascular endothelial growth factor (VEGF) (Fraser & Wulff 2001, Greenaway *et al.* 2005). This angiogenic growth factor seems to carry out in the ovary, as demonstrated in other tissues, three discrete roles in the control of vascular development: it is capable of initiating angiogenesis by promoting endothelial cell proliferation by chemoattraction (Fraser *et al.* 2000, Tamanini & De Ambrogi 2004), it maintains immature blood vessels viable (Goede *et al.* 1998) and it facilitates the process of pericyte recruitment as the final phenomenon of blood vessel maturation (Hirschi & D'Amore 1996, Beck & D'Amore 1997, Benjamin *et al.* 1998, Israely *et al.* 2003).

VEGF has been shown to be a critical molecule involved in the regulation of follicle development in different species (Barboni *et al.* 2000, Mattioli *et al.* 2001, Wulff *et al.* 2001, 2002, Berardinelli *et al.* 2002, Hunter *et al.* 2004). Recent studies have shown that it exerts a crucial role during the transition from preovulatory follicles to ovulation (Wulff *et al.* 2001, Zimmermann *et al.* 2003) but few data describe the production of VEGF during the passage from pre- to periovulatory follicles and what role it exerts. At the end of each ovarian cycle, in fact, dominant follicle(s), selected from a cohort of growing antral structures, undergo ovulation in response to the luteinizing hormone (LH) surge and, subsequently, ovulate and differentiate into corpus luteum (CL) (Greenwald & Terranova 1988). Dramatic changes in follicular morphology and vasculature are associated with the luteinization process. Capillary endothelial cells, localized in the vessels of the internal theca, rapidly proliferate and invade the avascular granulosa layers (Shimoda *et al.* 1993, Christenson & Stouffer 1997), forming a widespread capillary network to supply the proliferating luteal cells. The rate of cellular division of the early developing CL is extremely

DOI: 10.1677/jme.1.01921
0952–5041/06/036–107
Online version via http://www.endocrinology-journals.org

high, comparable with that observed in aggressive tumours (Reynolds *et al.* 2000). Consistent with this high CL growth rate is the rapid transition and reorganization of follicular into luteal vasculature. An increase in ovarian blood flow and hyperaemic changes, elicited by the LH surge, were first observed by Zondek *et al.* (1945). Changes in ovarian and follicular microcirculation have been quantified more recently by using immunohistochemical approaches (Murdoch & Dunn 1983, Abisogun *et al.* 1988) as well as transrectal colour Doppler ultrasonography (Acosta *et al.* 2003, 2004). This non-invasive technique allowed conformation of an impressive increase in the ovarian blood flow that starts during the periovulatory period and stabilizes in mature CL. The success of this process appears to be of vital importance for mammals, since the establishment and maintenance of pregnancy is strictly dependent on the development of a mature CL capable of producing high levels of progesterone (Hunter *et al.* 2004, Stouffer 2004).

Recent studies performed on rodents and primates have shown that CL formation is completely impaired by VEGF immunoneutralization obtained using soluble receptors or receptor-blocking antibodies (Wulff *et al.* 2001, 2002, Zimmermann *et al.* 2003).

If VEGF plays a crucial role even during the final phase of folliculogenesis, little is known of the local changes induced by this factor on follicle blood vessels after the LH surge. To this end, the present study was performed to describe the VEGF spatio-temporal expression pattern and the endothelial cell system involved in blood vessel remodelling during the periovulatory period in prepubertal gilts. In order to describe angiogenesis at a precise phase of follicle development (preovulatory and periovulatory periods), we have therefore adopted a validated hormonal treatment (Mattioli *et al.* 2001, Shimizu *et al.* 2002, Galeati *et al.* 2003) that induces follicle growth by using 1250 IU equine chorionic gonadotrophin (eCG) and stimulates ovulation with 750 IU human chorionic gonadotrophin (hCG).

The pig model was chosen for this research because of the long periovulatory interval (40–44 h) which facilitates the analysis of the temporal evolution of angiogenesis that precedes ovulation. Finally, in order to characterize the follicular vascular network, the recruitment of mural cells (i.e. pericyte or vascular smooth muscle cells) has been evaluated.

Materials and methods

Ovarian collection

Fifteen prepubertal Large White gilts weighing 90·7 ± 5·2 kg (mean ± S.D.) were injected i.m. with a single dose of 1250 IU eCG (Folligon; Intervet, Boxmeer, The Netherlands) to promote follicular growth in 60–72 h. The dose of eCG used to stimulate follicular growth was chosen according to several reports (Mattioli *et al.* 2001, Shimuzi *et al.* 2002, Galeati *et al.* 2003) since it guarantees a slight superovulatory treatment (Knox 2005). Ovulation was induced with hCG (Corulon; Intervet) treatment (750 IU, i.m.) carried out 60 h after eCG when more than 80% of the follicles have reached a preovulatory diameter (Barboni *et al.* 2000), and have activated steroidogenesis (Mattioli *et al.* 2001).

On the basis of the hormonal protocol, the treated animals were divided into three groups of five animals each, in order to obtain: preovulatory follicles, 60 h after eCG (control group), periovulatory follicles, 18 h after hCG and periovulatory follicles, 36 h after hCG.

Ovaries were recovered by laparotomy from anaesthetized animals by an injection of azaperone (6 ml/gilt; Stresnil; Janssen, Geerse, Belgium) and atropine sodium salt (2 mg/gilt; Industria Galenica Senese, Siena, Italy), and maintained under thiopenthal sodium (1·5 g/gilt; pentothal sodium; Gellini, Aprilia, Italy) anaesthesia (Barboni *et al.* 2000). All protocols had prior approval from the Ethical Committee of the University of Teramo.

All the ovaries used in the present study showed a uniform follicular response in terms of follicle size and number.

One ovary from each animal, immediately after removal, was fixed in 4% paraformaldehyde/phosphate-buffered saline (PBS; pH 7·4) for 12 h at 4 °C, dehydrated and embedded in paraffin wax. The contralateral ovary was collected to isolate single healthy follicles with a diameter >6 mm. The follicular wall obtained from each follicle was opened to collect follicular fluid (FF) and mechanically disaggregated to isolate the granulosa layer from the theca shells (Barboni *et al.* 2000, 2004, Mattioli *et al.* 2001, Berardinelli *et al.* 2002). FF, granulosa and theca samples were then individually frozen until western blot analysis.

VEGF assay

VEGF concentration in FF was quantified according to Barboni *et al.* (2000), using a specific ELISA (Quantikine; R&D Systems, Minneapolis, MN, USA) developed for the quantitative determination of VEGF in cell culture supernatant, serum and plasma. In brief, this highly specific sandwich assay recognizes human $VEGF_{165}$ as well as $VEGF_{121}$, whereas it exhibits negligible cross-reactivity with all other cytokines/growth factors tested. A 96-well plate reader (Biomek 1000; Beckman Instruments, Fullerton, CA, USA) set to read at an emission of 450 nm was used to quantify the results. Since the VEGF kit was manufactured to detect human VEGF, a test of parallelism was carried out to investigate whether the assay could also be reliably used to measure pig soluble VEGF isoforms, such as $VEGF_{164}$, which is

the prevalent isoform demonstrated in porcine ovaries (Barboni *et al.* 2000, Boonyaprakob *et al.* 2003, Shimizu *et al.* 2003). To this end, the standard curve generated with a highly purified S*f*-21-expressed recombinant human $VEGF_{165}$ (R&D Systems; 0, 62·5, 125, 250, 500 and 1000 pg/ml) was compared with a curve that was obtained from a sample of pig FF diluted with the appropriate calibrator solution provided with the kit, in order to produce samples with values that fell within the dynamic range of the assay. The two curves were perfectly parallel, thus showing that the system does not reveal any major difference between human and pig VEGF. The minimum detectable dose of the assay, obtained by adding 2 standard deviations to the mean optical density value of 20 standard replicates and calculating the corresponding concentration, was equivalent to 5 pg/ml FF. Intra- and interassay precision, expressed as the coefficient of variation for replicate determinations of a pooled FF sample, were 5·6% (16 replicates) and 7·8% (eight replicates) respectively.

For each sample of FF analyzed the VEGF assay was performed in two replicates. The levels of VEGF in FF samples are expressed as ng/ml FF. VEGF results are finally presented as means ± S.D. of the single follicle analysis for each hormonal treatment.

Western blot analysis

Immunoblotting was performed with two different antibodies: the monoclonal anti-human $VEGF_{165}$ (dilution 1:500; R&D Systems) used in the ELISA and, in parallel, the polyclonal anti-human VEGF-Ab2 (dilution 1:80; Oncogene, San Diego, CA, USA). Human recombinant $VEGF_{165}$ (R&D Systems) as well as mouse recombinant $VEGF_{164}$ (R&D Systems) were used to identify the band of the angiogenic factor and to co-localize the porcine VEGF that has a similar molecular weight (Shimizu *et al.* 2003).

Proteins were extracted from granulosa cells or theca layers of single follicles isolated from treated gilts or from CL (day 5–13) obtained from ovaries of untreated pigs collected at the slaughterhouse. Since the presence of $VEGF_{164}$ has been confirmed in porcine CL (Boonyaprakob *et al.* 2003), proteins collected from pooled CL were used as the positive control.

Briefly, the tissues were transferred into 5 volumes of extraction buffer: 20 mM Tris–HCl, pH 7·5, 1% Igepal, 0·1% dithiothreitol, 2 mM phenylmethylsulphonyl fluoride, 2 mM sodium orthovanadate, 10 mM sodium fluoride, 10 μg/ml leupeptin, 10 μg/ml antipain and 100 units/ml aprotinin (as phosphatase and protease inhibitors) (all the products were obtained from Sigma) and homogenized in an ice bath with a tissue homogenizer. Five bursts of 15 s at maximum speed with 45-s intervals of cooling between each burst were applied. The homogenate was then centrifuged at 2000 ***g*** for 15 min at 4 °C (Berisha *et al.* 2000). The supernatant was recovered and an aliquot was used to evaluate the amount of proteins by the method of Lowry *et al.* (1951).

Seventy-five micrograms of proteins were separated by 12% SDS-PAGE and then electrophoretically transferred to a nitrocellulose membrane (Hybon C Extra; Amersham Pharmacia, Piscataway, NJ, USA) for immunoblot analysis according to standard protocols (Towbin *et al.* 1979). For protein detection, the membranes were incubated with the primary antibodies. As secondary antibody, peroxidase-conjugated anti-mouse or anti-rabbit immunoglobulins (dilution 1:4000; Santa Cruz Biotechnology Inc, Santa Cruz, CA, USA) were used. After the stripping procedures (60 mM Tris–HCl, pH 6·8, 2%SDS and 100 mM β-mercaptoethanol at 60 °C for 45 min), the filter was reprobed with a monoclonal anti-α tubulin (dilution 1:5000; Sigma) and then with an anti-mouse secondary antibody. The signals were detected by using the ECL Western blot analysis system (Amersham Pharmacia). Seven different follicles/gilt were analyzed for the three hormonal treatments considered.

Quantitative data were determined as the mean ratio of the optical density of the specific bands normalized to that of α-tubulin. The densitometric analysis was carried out with the Advanced Image Data Analyzer (Rai Test; GMBH, Straubenhardt, Germany). Finally, to facilitate the interpretation of the quantitative data, VEGF protein levels were expressed as a fold increase over the mean densitometric content of VEGF recorded in granulosa cells treated with eCG; this was arbitrarily set at 1.

Histological investigation and analysis of data

Serial paraffin sections of 5 μm thickness were collected on poly-L-lysine-coated slides (Sigma). For morphological and morphometric analyses, a series of 20 sections at a distance of 100 μm/ovary was used. Serial sections were subjected to: (a) haematoxylin–eosin (HE) staining to identify healthy follicles, to assess the stage of follicle development and to localize the red blood cells in the analyzed blood vessels; (b) immunohistochemistry for the endothelial marker, von Willenbrand Factor (vWF); (c) a double immunolabelling technique for vWF and VEGF; (d) a double immunolabelling technique for vWF and Ki-67 antigen, a cell proliferation marker (Garrett & Guthrie 1997, Scolzen & Gerdes 2000); (e) a double immunolabelling technique for vWF and α-smooth muscle actin (α-SMA), a molecular marker for mural cells (Hirschi & D'Amore 1996, Redmer *et al.* 2001, Israely *et al.* 2003); (f) *in situ* hybridization to VEGF mRNA ($VEGF_{164}$).

For each hormonal treatment considered, the analyses were carried out on at least three healthy large antral follicles/ovary per gilt. In more detail, a total of 18

preovulatory follicles and 20 and 24 periovulatory follicles isolated 18 h and 36 h after hCG treatment respectively were considered.

A qualitative analysis was performed for all double immunolabelling procedures. Slides were inspected with an Axioscop 2 plus (Zeiss, Oberkochen, Germany) epifluorescence microscope equipped with an Axiovision Cam (Zeiss).

Quantitative analysis on tissue sections was performed using an image analysis system linked to a Zeiss camera and the data were processed using a KS300 computed image analysis system (Zeiss), as previously described (Barboni *et al.* 2004). In brief, sections were inspected at low magnification (× 100) to assess the stage of follicular development which was classified according to Wulff *et al.* (2002).

In this study, only healthy large antral follicles (diameter >6 mm) were analysed. Follicles were considered as healthy if they contained a normal-shaped oocyte surrounded by granulosa cells regularly apposed on an intact basement membrane, with normal appearance of their nuclei (without signs of picnosis; HE staining). Follicles not fulfilling these criteria were classified as unsuitable for analysis. The follicular diameter was then identified with the cumputed image analysis system (KS300; Zeiss) set up to measure two diameters of the follicle sections at a right angle. The mean follicular diameter was calculated from these measurements. Furthermore, for each morphometric analysis performed, at least two sections/follicle were randomly chosen and the whole cross-follicular wall was analysed.

Immunohistochemistry

vWF

The sections, after rehydrating, were kept in 2% hydrogen peroxide (Merck, Darmstadt, Germany) in methanol (Merck) for 5 min to remove endogenous peroxidase activity, and then washed with PBS. The slides were placed in citrate buffer (pH 6), antigen retrieval was performed by treating the sections in a hotbox oven (HO) at 95 °C for 5 min twice, and then washing in PBS. After normal goat serum (NGS; Sigma) blocking for 30 min to avoid non-specific binding, sections were incubated with the rabbit anti-vWF (Dako, Glostrup, Denmark) diluted 1:400 in PBS/1% bovine serum albumin (BSA) at room temperature overnight (RT-O/N). As secondary antibody, biotinylated-conjugated anti-rabbit immunoglobulins (1:100 in PBS/1% BSA; Sigma) were used. The immunoreaction was visualized using the avidin–biotin complex method and then with the 3–3′ diaminobenzidine–ammonium nickel sulphate method, according to Mattioli *et al.* (2001).

Human breast carcinoma tissue samples (Weidner *et al.* 1991), a kind gift from Dr De Carolis of the 'Giuseppe Mazzini' Hospital of Teramo, were used as a positive control. NGS was used as a negative control in place of primary antibodies.

To quantify the vascular area (VA) (i.e. vWF-positive cells), the section was measured at × 400 magnification. The captured grey scale image was thresholded and converted to a binary image. The VA was then given by the extension of the vWF-positive area in μm^2/15 000 μm^2 theca. The whole area of the theca compartment and the vWF-positive area within the compartment were measured (Barboni *et al.* 2004). The results are expressed as mean values ± S.D. for the number of follicles analysed within each follicular stage (Mattioli *et al.* 2001, Berardinelli *et al.* 2002, Barboni *et al.* 2004).

VEGF–vWF

This double immunostaining was performed according to the method of Polak & Van Noorden (1997). After inhibition of endogenous peroxidases and HO treatment, the sections were incubated first with NGS for 30 min and then with the rabbit anti-VEGF-Ab2 (Oncogene), the same antibody as that used in the Western blot analysis, diluted 1:10 in PBS/1% BSA at RT-O/N. As secondary antibody, biotinylated-conjugated anti-rabbit immunoglobulins (1:100 in PBS/1% BSA; Sigma) were used. This immunocomplex layer was detected using the TSA Fluorescein System (NEN Life Science Products, Hounslow, Essex, UK), according to the manufacturer's protocol. Furthermore, after washing in PBS, the same sections were incubated with NGS for 30 min and then with rabbit anti-vWF at RT-O/N. After washing in PBS, tissue sections were then processed with CY3-labelled secondary goat anti-rabbit antibody (diluted 1:100 in PBS and applied for 1 h; Sigma).

Human breast carcinoma tissue samples (Heffelfinger *et al.* 1999) were used as a positive control. NGS was used as a negative control in place of primary antibodies. The specificity of double immunostaining was verified by localizing each antigen separately.

Ki-67–vWF

This double immunostaining was performed according to the method of Polak & Van Noorden (1997). In order to identify proliferating endothelial cells after endogenous peroxidase inhibition and HO treatment, the slides were incubated with mouse anti-Ki-67 antibody at RT-O/N (clone MIB-1, diluted 1:75 in PBS/1% BSA; Dako). After biotinylated-conjugated anti-mouse immunoglobulins (1:100 in PBS/1% BSA; Sigma) the immunocomplex was detected by the TSA Fluorescein System (NEN Life Science Products). The same sections were then processed for vWF and visualized with fluorescent antibody as described above.

The tissue used as the positive control was a sample of human breast carcinoma (Bottini *et al.* 2001). NGS was used as a negative control in place of primary antibodies. The specificity of double immunostaining was verified by localizing each antigen separately.

α-SMA–vWF

This double immunostaining was performed according to the method of Polak & Van Noorden (1997). Mouse anti-α-SMA (diluted 1:500 in PBS/1% BSA; Oncogene) and rabbit anti-vWF (diluted 1:400 in PBS/1% BSA) were applied together at RT-O/N, after HO treatment. The tissue sections were then incubated with a mixture of differently labelled anti-rabbit and anti-mouse immunoglobulins: for the vWF immunocomplex layer a CY3-labelled secondary goat anti-rabbit antibody (1:100 in PBS; Sigma) was used while the α-SMA immunocomplex layer was visualized by using a fluorescein isothiocyanate (FITC)-labelled secondary goat anti-mouse antibody (diluted 1:100 in PBS and applied for 1 h; Sigma).

According to the data sheet instructions, bovine aorta tissue collected at the slaughterhouse was used as the positive control. NGS was used as a negative control in place of primary antibodies. The specificity of double immunostaining was verified by localizing separately each antigen.

Tissue sections were counterstained with DAPI (Vectastain, Burlingame, CA, USA). Fluorescent staining qualitative analysis was performed by taking a micrograph of the three fluorescent dyes (FITC, CY3 and DAPI) for each section. Successively, the sections were re-stained with HE and micrographs of the same fluorescent fields were performed to identify and subtract the red cells within each blood vessel analysed.

In situ hybridization

In situ hybridization was performed with a commercially available kit (HybriProbe kit; Biognostik, Göttingen, Germany). A custom-synthesized oligonucleotide double-FITC-labelled cDNA probe for porcine $VEGF_{164}$ was obtained from Biognostik. The design process of the oligonucleotide sequence was based on accession no. X81380 (porcine mRNA for VEGF). The probe sequence (5′–3′) was as follows: 5′-CAC GTC TGC GGA TCT TGT ACA AAC AAA TGC-3′ (Barboni *et al.* 2004).

Ovarian tissue sectioning was performed in RNase-free water at 7 μm, as suggested by the Biognostik HybriProbe kit manual, and then sections were mounted on poly-L-lysine-coated slides, dewaxed and rehydrated. Quenching of endogenous peroxidase was performed by 3% H_2O_2 in PBS for 10 min and then tissue sections were treated with proteinase K (20 μg/ml in 50 mM Tris–HCl (pH 7·4) containing 50 mM EDTA and 10 mM NaCl) for 15 min at 37 °C. Sections were prehybridized for 4 h at 30 °C with 25 μl hybridization buffer supplied with the probe. The sections were then hybridized overnight at 30 °C with the cDNA probe at 60 pmol/ml in hybridization buffer. Post-hybridization washes included 2 × 5 min in 1 × SSC and 2 × 15 min in 0·1 × SSC at 39 °C (Barboni *et al.* 2004).

The FITC-labelled probe was detected using the TSA Fluorescein System (NEN Life Science Products), as described above. As the negative control, sections were treated with a random double-FITC-labelled oligonucleotide probe containing the same proportion of cytosine and guanine bases as the VEGF probe supplied by the manufacturer.

In situ hybridization quantification was carried out by counting the number of positive cells within the outlined compartment of interest. To identify the VEGF mRNA-expressing cells the sample was measured at × 400 magnification, the image was then captured in grey scale, thresholded and converted to a binary image, and the results are expressed as positive cells per unit area (15 000 μm^2) calculated individually for theca and granulosa compartments, according to Barboni *et al.* (2004). VEGF mRNA expression was calculated as a mean value ± S.D. for the number of follicles assessed within the different hormonal treatments (Barboni *et al.* 2004).

Statistical analysis

The quantitative data obtained from the different hormonal treatments were assessed by the Kurtosi test. Successively, the values were compared using ANOVA and Student's *t*-test, and were considered significant when $P<0·05$.

Results

Ovarian response to hormonal treatment

The population of follicles isolated from treated ovaries of prepubertal gilts displayed a uniform response as previously described (Barboni *et al.* 2000). In fact, 60 h after eCG treatment the mean number of large antral follicles (diameter >6 mm) recorded was 20·98 ± 4·05/animal (means ± S.D.). In hCG-stimulated gilts the mean number of large antral follicles (diameter >6 mm) recruited was 23·15 ± 3·71/animal and 24·68 ± 6·01/animal at 18 h and 36 h later respectively.

VEGF in FF

Administration of hCG induced a progressive reduction of VEGF levels in the FF that fell from values of 11·45 ± 2·01 ng/ml (60 h after eCG, $n=34$) to

0·40 ± 0·28 ng/ml (n=31, P<0·05) and undetectable levels (not defined, n=29) at 18 h and 36 h after hCG respectively.

VEGF immunoblot analysis

As shown in Fig. 1, the immunoblot analysis performed with the antibody utilized previously for the ELISA revealed that granulosa cells in the control group (60 h after eCG) showed similar VEGF levels to those present in theca layers. Administration of hCG (periovulatory follicles 18 h after hCG) induced a transient and significant decrease (P<0·05) in protein content in granulosa layers followed, 36 h later, by a new accumulation of VEGF (P<0·05).

Unchanged VEGF levels in the theca layers were recorded 18 h after hCG injection vs the control group, while high levels of the protein (P<0·05) were revealed close to the time of ovulation. A similar VEGF pattern was obtained by re-probing the filters with the VEGF polyclonal antibody.

In situ hybridization

In preovulatory follicles, VEGF mRNA was recorded in approximately 90% of granulosa cells (19·65 ± 4·61 cells/unit area). hCG administration did not change the VEGF mRNA content in the granulosa layer where 16·98 ± 5·99 and 20·50 ± 8·71 positive cells/unit area were recorded 18 h and 36 h later respectively (Fig. 2).

In preovulatory follicles (60 h after eCG), only a few theca cells were hybridized to the probe (3·95 ± 2·59 cells/unit area), while VEGF mRNA-positive cells progressively increased after hCG treatment. In detail, 6·40 ± 3·85 (P>0·05) and 18·33 ± 6·32 (P<0·01) positive theca cells/unit area were recorded 18 h and 36 h after hCG stimulation respectively (Fig. 2).

vWF labelling

Blood vessels architecture is illustrated in Fig. 3 and quantified in Fig. 4. Preovulatory follicles have two concentric networks connected to each other by anastomotical vessels: an inner one laying directly on the basal membrane and an outer network localized within the external theca.

The total VA recorded was 6746·17 ± 1339·72 VA/field area, and the outer network accounting for most of the area was 3863·71 ± 799·56 VA/field area. Eighteen hours after hCG administration, the follicles showed a marked decrease in the extension of the total VA (3822·13 ± 828·74 VA/field area, P<0·05) caused by a dramatic decrease in the outer network (1068·96 ± 175·64 VA/field area, P<0·01).

Close to ovulation (36 h after hCG), the total VA significantly increased again and reached an extension higher than that recorded in preovulatory follicles (8623·70 ± 2983·01 VA/field area, P<0·01). While the inner network was unaltered (2859·26 ± 275·85 VA/field area, P>0·05), the outer network reached approximately 60% of the total VA (5764·44 ± 1001·64 VA/field area, P<0·01).

vWF and VEGF

The double-labelling procedure allowed us to identify endothelial cells (vWF-positive cells; red stain), VEGF protein (green stain) and to co-localize both molecular markers (yellow stain) (Fig. 3). Preovulatory follicles showed the endothelial cells organized in two concentric networks, and displayed VEGF immunopositivity in the majority of granulosa cells and in the theca layer. No cells co-localized both markers.

Eighteen hours after hCG, the follicular wall displayed an inner network and a reduced outer one. The cellular VEGF content fell in both follicle compartments while the protein started to be accumulated in the extracellular matrix of the theca layer. In the theca compartment, single large cells that co-localized vWF and VEGF without any relationship with blood vessels were observed.

Thirty-six hours after hCG, a profound vascular reorganization was observed: the anastomotical vessels, running in the projections toward the antrum cavity of inner theca, increased their lumina. For the first time, large blood vessels appeared in the follicle wall. Cells of the inner microvasculature close to the basal membrane, as well as of the outer network, co-localized VEGF and vWF.

vWF and Ki-67

The simultaneous staining for vWF (red stain) and Ki-67 (green stain) was used to identify the proliferating endothelial cells during the different follicular stages (Fig. 5). Preovulatory follicles displayed proliferating endothelial cells either in the inner or in the outer vascular network. In fact, some vWF-positive endothelial cells simultaneously showed nuclei labelled with Ki-67. Periovulatory follicles, 18 h after hCG, displayed a reduced extension of the total VA, and a low proliferating status of the endothelial cells. Moreover, single round cells that co-localized Ki-67 and vWF were occasionally recorded in theca layers. Close to ovulation, dual-stained cells were observed either in the microvessels of the inner network or in the large blood vessels of the outer one.

vWF and α-SMA

vWF (red stain) and α-SMA (green stain) double-labelling procedure was performed in order to classify the follicular blood vessels (Fig. 6). In pre- and

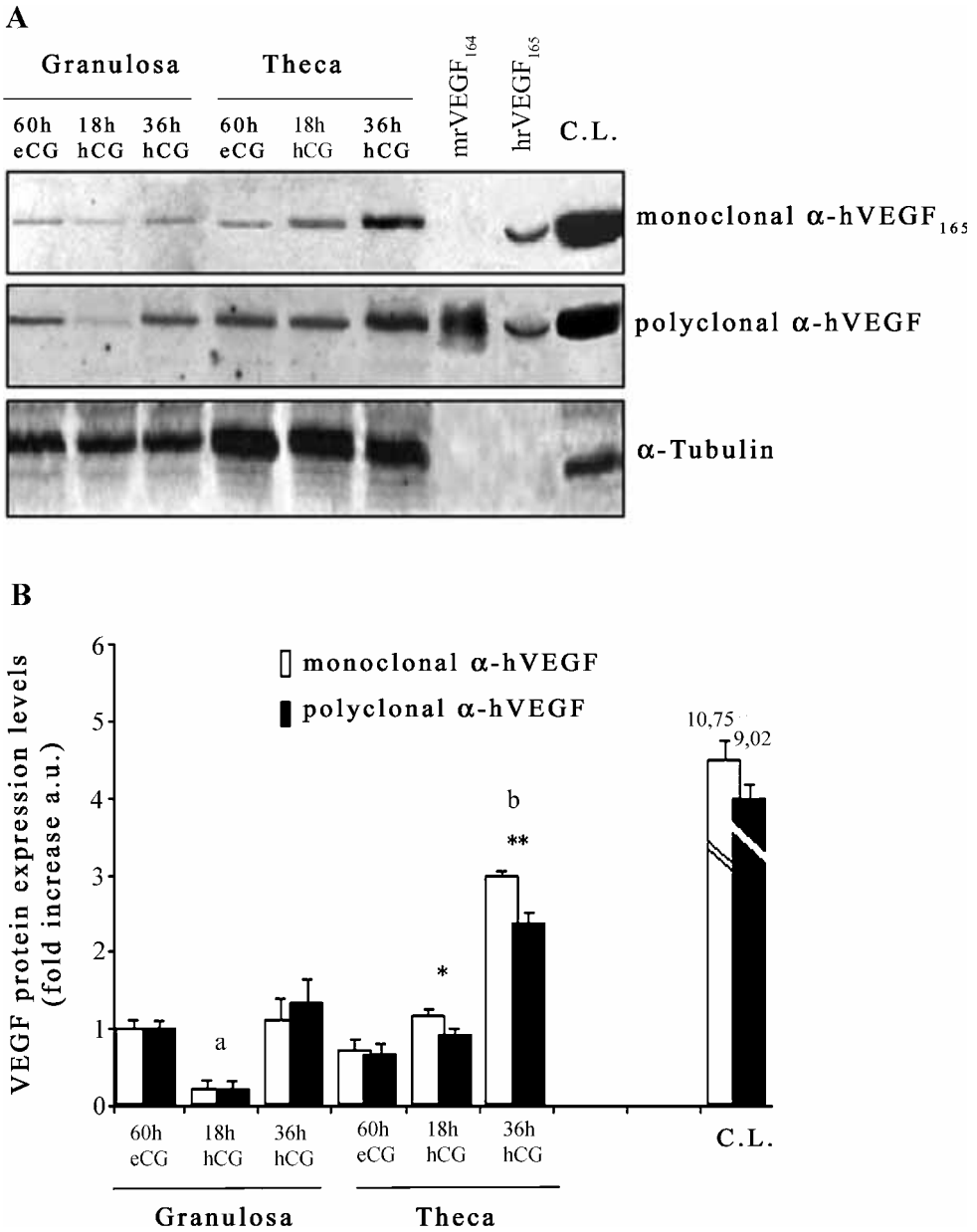

Figure 1 VEGF protein content in granulosa and theca compartments of pre- and periovulatory follicles. (A) Representative immunoblots carried out on equal amounts (75 μg) of protein extracted from granulosa cells or theca layers of large follicles isolated from treated prebubertal gilts (60 h eCG, 18 h and 36 h hCG) and from pig CL (days 5–13, positive control) obtained from ovaries collected at the slaughterhouse. The immunoblotting was performed by using a monoclonal anti (α)-human (h) $VEGF_{165}$ antibody (top), a polyclonal anti-human VEGF antibody (middle) and an anti-tubulin antibody (bottom) to normalize the results. The mouse recombinant (mr) $VEGF_{164}$, human recombinant (hr) $VEGF_{165}$ and lysates of porcine CL were loaded as positive controls. (B) The graph indicates the VEGF level determined as the mean ratio±S.D. of the optical density normalized to that of α-tubulin. The data were obtained by analysing a single follicular compartment of seven follicles/gilt. The values are expressed as fold increase over the mean densitometric content of VEGF recorded in granulosa cells treated with eCG that are arbitrarily set at 1. [a] The VEGF value recorded 18 h after hCG was significantly different from the other hormonal treatment in the granulosa compartment ($P<0{\cdot}05$). [b]The VEGF value recorded 36 h after hCG was significantly different from the other hormonal treatment in the theca compartment ($P<0{\cdot}05$). *The VEGF value recorded in the theca layer 18 h after hCG was significantly different from the level of the protein recorded in the granulosa compartment ($P<0{\cdot}05$). **The VEGF value recorded in the theca layer 36 h after hCG was significantly different from the level of the protein recorded in the granulosa compartment ($P<0{\cdot}05$). a.u., arbitrary units.

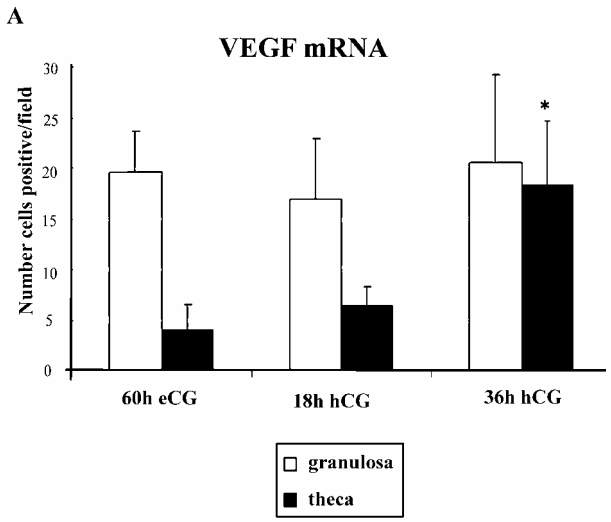

Figure 2 *In situ* hybridization to VEGF mRNA in pre- and periovulatory follicles. (A) Quantitative analyses were carried out by counting the number of positive cells within a unit area (15 000 μm^2) calculated individually for the theca (solid bars) and the granulosa (open bars) compartment in each follicle (60 h after eCG, n=18; 18 h after hCG, n=20; 36 h after hCG, n=24). VEGF mRNA content was then expressed as mean positive cells±S.D. for the number of follicles analysed within the different hormonal treatment. *Significantly different within each follicular compartment ($P<0{\cdot}01$). (B) An example of VEGF mRNA hybridization pattern in the theca compartment and its negative control (left). The negative control was performed with random double-FITC-labelled oligonucleotide probe containing the same proportion of cytosine and guanine bases as the VEGF probe (right). Bar=10 μm.

periovulatory follicles, 18 h after hCG injection, endothelial cells did not co-localize α-SMA either in the inner or in the outer vascular networks. Only large vessels that run out of the external theca displayed a

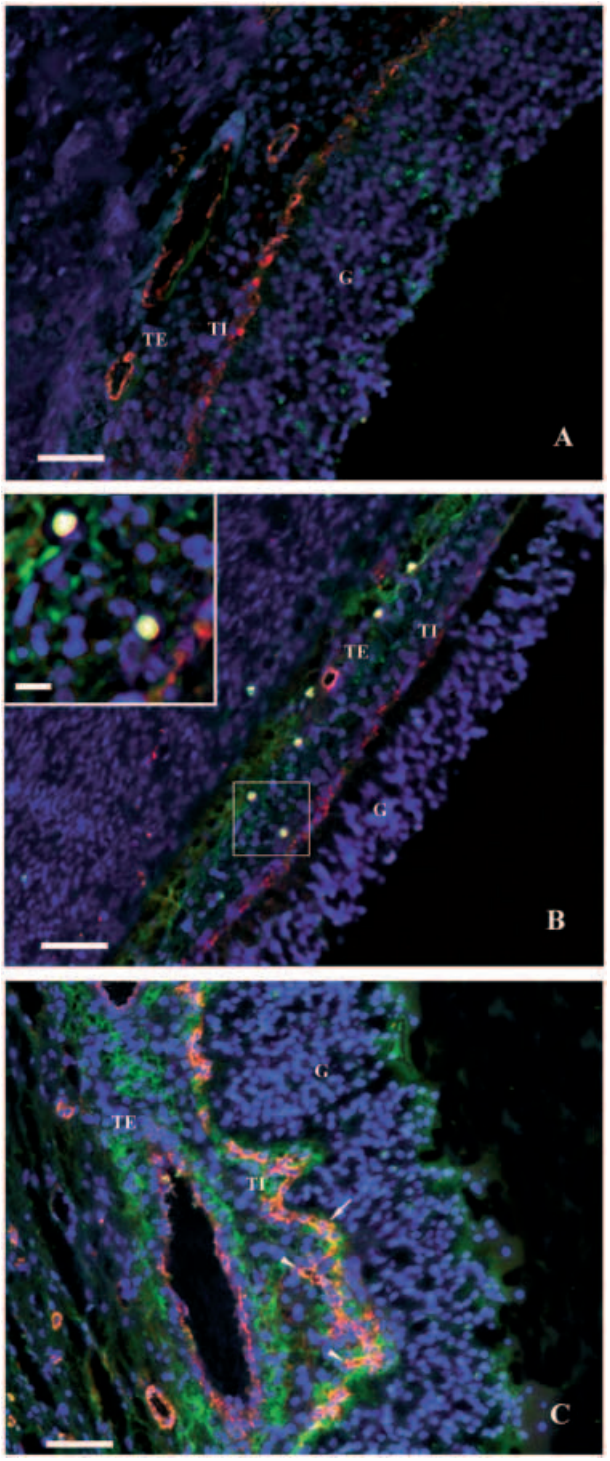

Figure 3 A representative example of double immunohistochemical localization of vWF (red stain) and VEGF (green stain). (A) Preovulatory follicles isolated 60 h after eCG (n=18) and periovulatory follicles isolated (B) 18 h (n=20) and (C) 36 h (n=24) after hCG. Nuclei were counterstained with DAPI (blue stain) to visualize the tissue morphology and to identify the follicular compartments (G=granulosa compartment; TI and TE=inner and outer theca compartment respectively). The insert panel visualizes cells co-localizing VEGF and vWF (yellow stain). Arrows and arrow heads indicate endothelial cells that co-localized VEGF in the inner and outer networks respectively. Bar=150 μm. Insert panel: bar=25 μm.

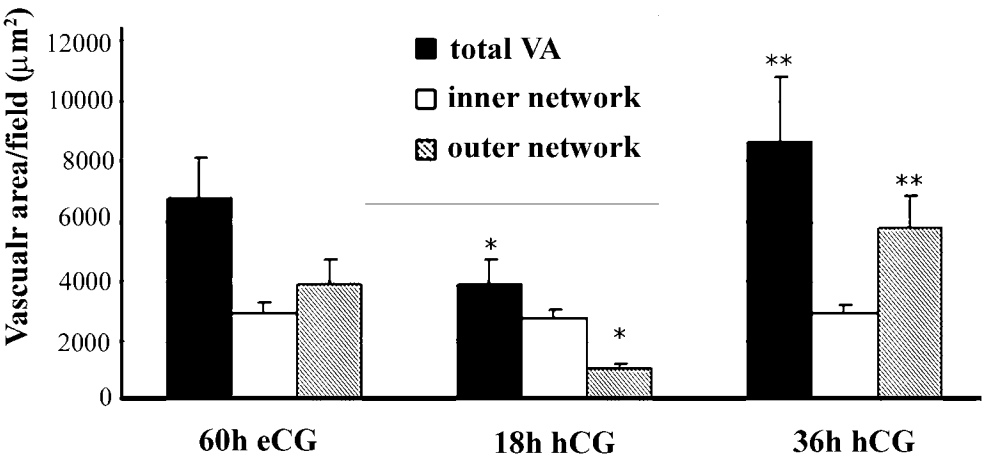

Figure 4 vWF immunostaining performed on pre- and periovulatory follicles. The quantitative analyses were carried out on preovulatory follicles (60 h after eCG, *n*=18), and on periovulatory follicles isolated 18 h (*n*=20) and 36 h (*n*=24) after hCG. The VA was given by the extension of vWF-positive area/15 000μm² of theca area. The results were calculated as total VA (solid bars), inner network (open bars) and outer network (shaded bars). The data are expressed as mean values±S.D. for the number of follicles analysed within each hormonal treatment. *, **Significantly different amongst total VA, inner or outer network recorded in each hormonal treatment ($P<0{\cdot}05$).

mural α-SMA positivity. Some single cells in the wall of periovulatory follicles 18 h after hCG displayed double staining for vWF and α-SMA.

The vascular organization was profoundly modified 36 h after hCG stimulation. In fact, the inner blood vessel network displayed vWF-positive cells that co-localized α-SMA. These cells are in direct contact with the underlying endothelial cells. Moreover, α-SMA-positive endothelial cells were observed in the large blood vessels of the outer network; in addition, widespread α-SMA immunopositivity was recorded at their periphery.

Discussion

The present research was performed to study the spatio-temporal expression pattern of VEGF in parallel with the analysis of endothelial cell proliferation and reorganization in order to understand the role exerted by this angiogenic factor in pig ovarian follicles after the LH surge. These data indicated for the first time that hCG treatment induces a new window of plasticity of blood vessel architecture in periovulatory follicles.

During the early hours after hCG, antral follicles showed a dramatic reduction in VEGF synthesis in the granulosa compartment accompanied by a parallel arrest of endothelial cell proliferation. As a consequence, a reduction in blood vessel extension was recorded, in agreement with a similar vascular remodelling observed by Cavender & Murdoch (1988) in sheep. However, the reduction of the follicular VA was not generalized and did not involve the inner network. The persistence of the inner capillary network is of vital importance for the follicles (Moor & Seamark 1986, Barboni *et al.* 2000, Mattioli *et al.* 2001) since it must guarantee a correct trophic supply of oxygen and metabolites to the avascular granulosa compartment and to the germinal cell. This role, hypothesized in the past by Moor & Seamark (1986), has recently been confirmed by the evidence that the follicular vasculature and the dissolved oxygen content in FF are positively related to oocyte developmental competence in humans (Sutton *et al.* 2003).

The inhibitory effect of the LH surge on the follicular VEGF content seems to be dependent on the progressive reduction of VEGF synthesis and secretion. Immunohistochemistry and Western blot analysis performed 18 h after hCG treatment revealed, in fact, a significant reduction in protein level in the granulosa layer. Nevertheless, VEGF mRNA content remained unchanged in the granulosa layer thus suggesting, as demonstrated in other tissue models, a post-transcriptional regulation of VEGF expression that occurs at the level of splicing, mRNA stability and translation (Neufeld *et al.* 1999). This modality of regulation has also been suggested in macaque granulosa cells, where a similar divergence in VEGF mRNA expression and protein production was observed (Hazzard *et al.* 1999). Moreover, since VEGF mRNA maintains a high level of stability within tissues (Neufeld *et al.* 1999) while the protein content is very variable in the ovarian follicles, a possible contribution of protein turnover, as well as the relative process of secretion that appears to be clearly dependent on gonadotrophin stimulation, cannot be excluded. In fact, VEGF levels in FF fell in periovulatory follicles after hCG stimulation.

The LH/hCG surge, in addition, was able to modify the pattern of VEGF secretion in the follicular compartments. The angiogenic factor progressively disappeared from the FF and started to be accumulated in the extracellular spaces amongst theca and granulosa cells. This observation seems to suggest a different solubility of the protein secreted in the periovulatory phase. The production of VEGF isoforms with high molecular weight (i.e. VEGF $-_{189}$), characterized by a lower solubility, could explain these results, as demonstrated in the endometrium when it is stimulated by a modified steroid milieu (Ancelin *et al.* 2002). In addition, it cannot be excluded that a change in the local heparin concentration or in the composition of cell surface heparan sulphate may condition VEGF bioavailability in the follicle (Robinson & Stringer 2001).

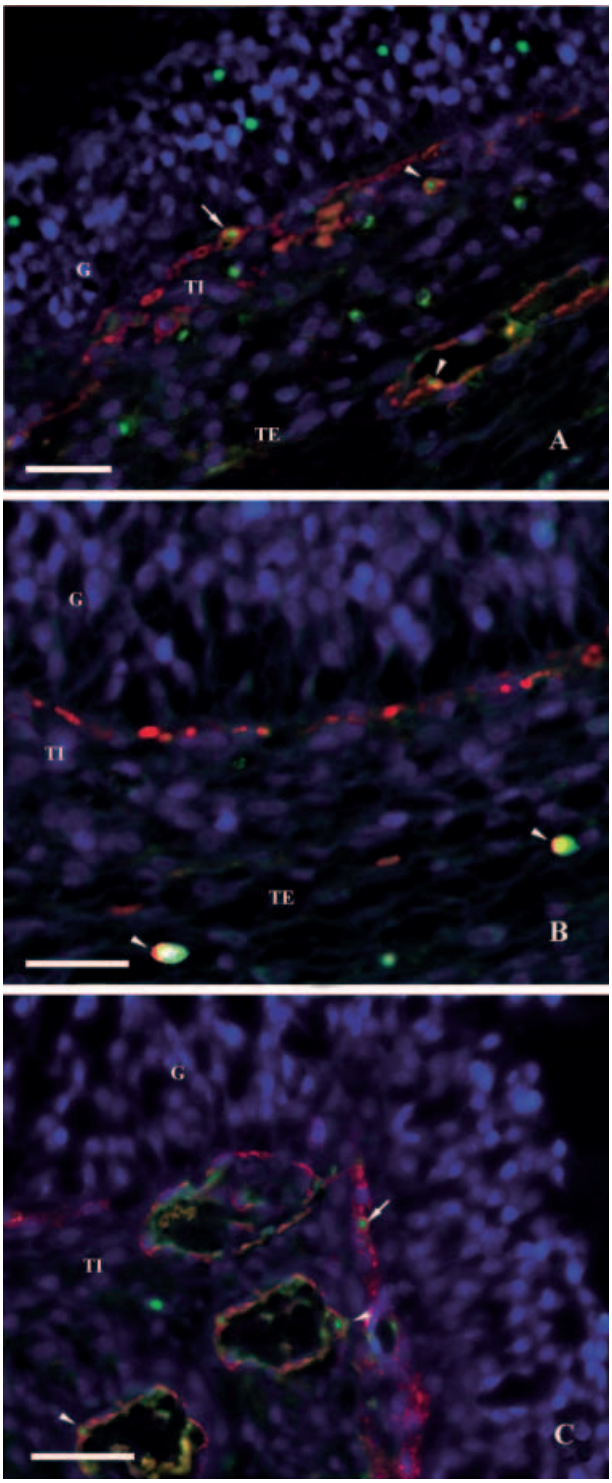

These periovulatory follicles displayed single cells characterized by an active status of proliferation that co-expressed vWF, VEGF and α-SMA. On the basis of their positivity these cells could be identified as mural cells (Gordon *et al.* 1996, Murata *et al.* 1996, Redmer *et al.* 2001). These cells appeared in the follicular wall for the first time. The blood vessel network recorded in preovulatory follicles is, in fact, composed of a homogenous web of endothelial cell tubes without any association with mural components.

In other tissues, such as the retina, the vasculature was initially organized in the endothelial plexus without pericyte coating and Benjamin *et al.* (1998) hypothesized that this interval determines a plasticity window for the vasculature to be remodelled and adjusted to the physiological needs of the tissue. Actually, the preovulatory follicle may be considered as a transitory structure whose morphological and functional evolution is strictly related to the LH surge. In addition, this transient stage of vascular immaturity may represent a prerequisite for blood vessel remodelling in periovulatory follicles.

The presence of mural cells in periovulatory follicles raises two important questions: what is the source of mural cells and what is their role during follicular development?

Despite increasing reports suggesting that mural cells are involved in maturation, remodelling and maintenance of the vascular system, little is known about their origin and recruitment. It has been hypothesized that mural cells are generated by *in situ* differentiation of mesenchymal precursors at the time of endothelial sprouting (Nehls *et al.* 1992). Other studies using an

Figure 5 A representative example of double immunohistochemical localization of the endothelial cell marker, vWF (red stain) and of the cell proliferation marker, Ki-67 antigen (green stain). Nuclei were counterstained with DAPI (blue stain) to visualize the tissue morphology and to identify the follicular compartments (G=granulosa compartment; TI and TE=inner and outer theca compartment respectively). The analysis was carried out on (A) preovulatory follicles (60 h after eCG, *n*=18) and periovulatory follicles isolated (B) 18 h (*n*=20) and (C) 36 h (*n*=24) after hCG. Arrows and arrow heads indicate endothelial cells that co-localized Ki-67 in the inner and outer networks respectively. Bar=75 μm.

'*in vitro* angiogenesis system' have suggested that pericytes are formed by migration and de-differentiation of arterial smooth muscle cells (Nicosia & Villaschi 1995). In our model, the mural cells recruited after the LH surge seemed to migrate into the follicular wall without any apparent association with pre-existing capillaries or vascular vessels.

Four to eight hours before ovulation (36 h after hCG) the follicular wall displayed a rapid and dramatic neovascularization. In parallel, theca and granulosa compartments started to synthesize new VEGF and to accumulate high levels of the protein within the extracellular matrix. During this final phase of follicular development, VEGF synthesis seems to involve both follicular compartments, while VEGF mRNA expression significantly increased only within the theca layer.

In order to understand the role of VEGF on the control of ovarian angiogenesis, a detailed investigation of both soluble and membrane-embedded receptors is required. Actually, the expression and localization of pig VEGF receptors have been analyzed during the follicular growth phase (Shimizu *et al.* 2002) and in CL (Boonyaprakob *et al.* 2003). No information, on the contrary, is available during the transition from the preovulatory to the periovulatory follicular stage.

In periovulatory follicles, high expression of VEGF was correlated with the presence of blood vessels characterized by a high degree of endothelial cell proliferation associated with the appearance of a large number of endothelial cells that co- expressed VEGF or α-SMA in the inner and outer networks.

The mural cells showed a different destiny in the two networks. On the basis of α-SMA and vWF co-expression (Nehls *et al.* 1992, Redmer *et al.* 2001) and their location within microvessels, mural cells distributed along the inner network can be classified as pericytes (Nehls *et al.* 1992). As shown in other tissues, pericyte processes penetrate the basement membrane to directly contact the underlying endothelium and, in a reciprocal manner, endothelial processes penetrate into the pericytes (Tilton *et al.* 1979) as also observed in the inner network of periovulatory follicles.

This observation seems to confirm previous reports by Redmer *et al.* (2001) that demonstrated the presence of pericytes during the transition from follicle to CL in the sheep. They revealed that pericytes are the first cells to

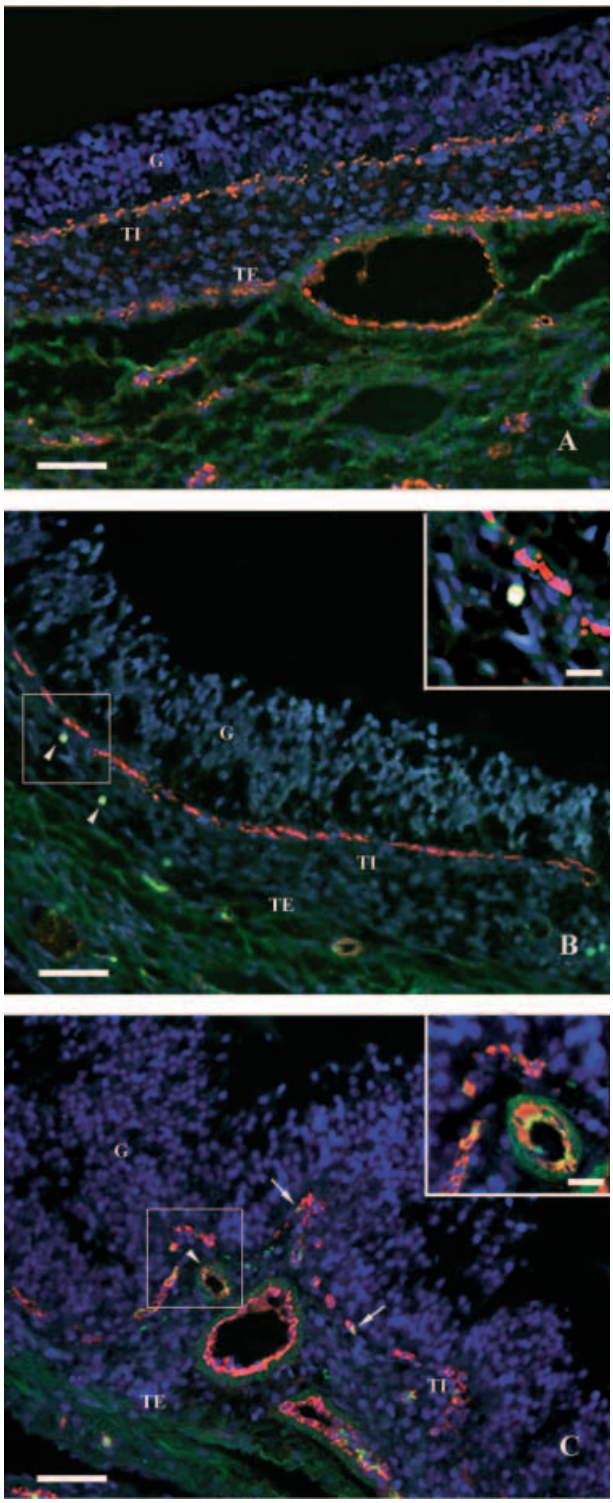

Figure 6 A representative example of double immunohistochemical localization of vWF (red stain) and of α-SMA, the smooth muscle actin/mural cell antigen (green stain). (A) preovulatory follicles isolated 60 h after eCG (*n*=18) and periovulatory follicles isolated (B)18 h (*n*=20) and (C) 36 h (*n*=24) after hCG. Nuclei were counterstained with DAPI to visualize the tissue morphology and to easily identify follicular compartments (G=granulosa compartment; TI and TE=inner and outer theca compartment respectively). The insert panels visualize cells that co-localized α-SMA and vWF. Arrows and arrow heads indicate endothelial cells that co-localized α-SMA in the inner and outer networks respectively. Bar=150 μm. Insert panel: bar=35 μm.

migrate into the follicular cavity from inner vessels after ovulation. With their ability to secrete VEGF these cells may contribute to the angiogenic process in the early CL (Redmer *et al.* 2001).

On the contrary, the mural cells observed in the outer network further differentiated into vascular smooth muscle cells, thus contributing to the structure of larger blood vessels that, for the first time, were detected in the typical theca projections toward the antrum. Vascular architecture was completely reorganized before ovulation. An active process of endothelial cell proliferation, recorded 36 h after hCG injection, increased the extension of the follicular blood vessel network and supported the development of large vessels in the theca, classifiable as arterioles or venules. The presence of smooth muscle in the vasculature in the theca compartment suggests that the nervous system or local mediators may contribute to the control of ovarian function by modulating follicle wall blood flow. This intense and rapid vascular remodelling, recorded a few hours before ovulation, was temporally associated with a resumption of VEGF production in both theca and granulosa compartments.

The present work confirms that, in the pig, hCG stimulation inhibits VEGF (Barboni *et al.* 2000). However the re-activation of VEGF started again some hours before ovulation. This wide blood vessel remodelling, revealed by the combined spatio-temporal description of the VEGF expression pattern and the analysis of endothelial cell organization, may have a crucial importance for follicle ovulation and successful CL formation. In fact, several reproductive pathological syndromes have been correlated to an abnormal expression of VEGF. In particular, high levels of VEGF are involved in the pathogenesis of ovarian hyperstimulation and polycystic ovary syndromes (Ferrara *et al.* 2003). In addition, low production of VEGF can generate infertility as demonstrated in some conditions of anovulation or early pregnancy loss (Geva *et al.* 2000).

Acknowledgements

We would like to thank Dr Delia Nardinocchi, Dr Oriana Di Giacinto and Dr Maura Turriani for technical assistance. The work was supported by Cofinanziamento miur Es. FIN 2004. The authors declare that there is no conflict of interest that would prejudice the impartiality of this scientific work.

References

Abisogun AO, Daphna-Iken D, Reich R, Kranzfeider D & Tsafriri A 1988 Modulatory role of eicosanoids in vascular changes during the preovulatory period in rat. *Biology of Reproduction* **38** 756–762.

Acosta TJ, Hayashi KG, Ohtani M & Miyamoto A 2003 Local changes in blood flow within the preovulatory follicle wall and early corpus luteum in cows. *Reproduction* **125** 759–767.

Acosta TJ, Gastal EL, Gastal MO, Beg MA & Ginther OJ 2004 Differential blood flow changes between the future dominant and subordinate follicles precede diameter changes during follicle selection in mares. *Biology of Reproduction* **71** 502–507.

Ancelin M, Buteau-Lozano H, Meduri G, Osborne-Pellegrin M, Sordello S, Plouet J & Perrot-Applanat M 2002 A dynamic shift of VEGF isoforms with a transient and selective progesterone-induced expression of VEGF189 regulates angiogenesis and vascular permeability in human uterus. *PNAS* **99** 6023–6028.

Barboni B, Turriani M, Galeati G, Spinaci M, Bacci ML, Forni M & Mattioli M 2000 Vascular endothelial growth factor production in growing pig antral follicles. *Biology of Reproduction* **63** 858–864.

Barboni B, Martelli A, Berardinelli P, Russo V, Turriani M, Bernabò N, Lucidi P & Mattioli M 2004 Ovarian follicle vascularization in fasted pig. *Theriogenology* **62** 943–957.

Beck L & D'Amore PA 1997 Vascular development: cellular and molecular regulation. *Journal of the Federation of American Societies for Experimental Biology* **11** 365–373.

Benjamin LE, Hemo I & Keshet E 1998 A plasticity window for blood vessel remodelling is defined by pericyte coverage of the preformed endothelial network and is regulated by PDGF-B and VEGF. *Development* **125** 1591–1598.

Berardinelli P, Martelli A, Russo V, Nardinocchi D, Turriani M, Barboni B, Mattioli M, Scapolo PA & Clavenzani P 2002 Correlation between VEGF production and blood vessels density in steroidogenic actvated pig antral follicles. *Italian Journal of Anatomy and Embryology* **107** 115–126.

Berisha B, Schams D, Kosman M, Amselgruber W & Eispainer R 2000 Expression and localisation of vascular endothelial growth factor and basic fibroblast growth factor during the final growth of bovine ovarian follicles. *Journal of Endocrinology* **167** 371–382.

Bjersing L & Cajander S 1974 Ovulation and mechanism of follicle rupture. VI. Ultrastructure of theca interna and the inner vascular network surrounding rabbit Graafian follicle prior to induced ovulation. *Cell and Tissue Research* **153** 31–44.

Boonyaprakob U, Gadsby JE, Hedgpeth V, Routh P & Almond GW 2003 Expression and localization of vascular endothelial growth factor and its receptors in pig corpora lutea during the oestrous cycle. *Reproduction* **126** 393–405.

Bottini A, Berruti A, Bersiga A, Brizzi MP, Bruzzi P, Aguggini S, Brunelli A, Bolsi G, Allevi G, Generali D, Betri E, Bertoli G, Alquati P & Dogliotti L 2001 Relationship between tumour shrinkage and reduction in Ki67 expression after primary chemotherapy in human breast cancer. *British Journal of Cancer* **19** 1106–1112.

Cavender JL & Murdoch WJ 1988 Morphological studies of the microcirculatory system of periovulatory ovine follicles. *Biology of Reproduction* **39** 989–997.

Christenson LK & Stouffer RL 1997 Follicle-stimulating hormone and luteinizing hormone/chorionic gonadotropin stimulation of vascular endothelial growth factor production by macaque granulosa cells from pre- and periovulatory follicles. *Journal of Clinical Endocrinology and Metabolism* **82** 2135–2142.

Ferrara N, Gerber HP & LeCouter J 2003 The biology of VEGF and its receptors. *Nature Medicine* **9** 669–676.

Fraser HM & Wulff C 2001 Angiogenesis in the primate ovary. *Reproduction, Fertility and Development* **13** 557–566.

Fraser HM, Dickson SE, Lunn SF, Wulff C, Morris KD, Carroll VA & Bicknell R 2000 Suppression of luteal angiogenesis in primate after neutralization of vascular endothelial growth factor. *Endocrinology* **141** 995–1000.

Galeati G, Spinaci M, Govoni N, Zannoni A, Fantinati P, Seren E & Tamanini C 2003 Stimulatory effects of fasting on vascular endothelial growth factor (VEGF) production by growing pig ovarian follicles. *Reproduction* **126** 647–652.

Garrett WM & Guthrie HD 1997 Steroidogenic enzyme expression during preovulatory follicle maturation in pigs. *Biology of Reproduction* **56** 1424–1431.

Geva E & Jaffe RB 2000 Role of vascular endothelial growth factor in ovarian physiology and pathology. *Fertility and Sterility* **74** 429–438.

Goede V, Schmidt T, Kimmina S, Kozian D & Augustin HG 1998 Analysis of blood vessels maturation processes during cyclic ovarian angiogenesis. *Laboratory Investigation* **78** 1385–1394.

Gordon JD, Mesiano S, Zaloudek CJ & Jaffe RB 1996 Vascular endothelial growth factor localization in human ovary and Fallopian tubes: possible role in reproductive function and ovarian cyst formation. *Journal of Clinical Endocrinology and Metabolism* **81** 353–359.

Greenaway J, Gentry PA, Feige JJ, Lamarre J & Petrik JJ 2005 Thrombospondin and vascular endothelial growth factor are cyclically expressed in an inverse pattern during bovine ovarian follicle development. *Biology of Reproduction* **72** 1071–1078.

Greenwald GD & Terranova PF 1988 Follicular selection and its control. In *The Physiology of Reproduction*, pp 439–445. Eds E Knobil & J Neill. New York: Raven Press.

Hazzard TM, Molskness TA, Chaffin CL & Stouffer RL 1999 Vascular endothelial growth factor (VEGF) and angiopoietin regulation by gonadotrophin and steroids in macaque granulosa cells during the peri-ovulatory interval. *Molecular Human Reproduction* **5** 1115–1121.

Heffelfinger SC, Miller MA, Yassin R & Gear R 1999 Angiogenic growth factors in preinvasive breast disease. *Clinical Cancer Research* **5** 2867–2876.

Hirschi KK & D'Amore PA 1996 Pericytes in the microvasculature. *Cardiovascular Research* **32** 687–698.

Hunter MG, Robinson RS, Mann GE & Webb R 2004 Endocrine and paracrine control of follicular development and ovulation rate in farm species. *Animal Reproduction Science* **82–83** 461–477.

Israely T, Dafni H, Granot D, Nevo N, Tsafriri A & Neeman M 2003 Vascular remodelling and angiogenesis in ectopic ovarian transplants: a crucial role of pericytes and vascular smooth cells in maintenance of ovarian grafts. *Biology of Reproduction* **68** 2055–2064.

Jiang JY, Macchiarelli G, Tsang BK & Sato E 2003 Capillary angiogenesis and degeneration in bovine ovarian antral follicle. *Reproduction* **125** 211–223.

Knox RV 2005 Recruitment and selection of ovarian follicles for determination of ovulation rate in the pig. *Domestic Animal Endocrinology* **29** 385–397.

Lowry OH, Rosebrough NJ, Farr AL & Randall RJ 1951 Protein measurement with the Folin Pheno reagent. *Journal of Biological Chemistry* **193** 265–275.

Mattioli M, Barboni B, Turriani M, Galeati G, Zannoni A, Castellani G, Berardinelli P & Scapolo PA 2001 Follicle activation involves vascular endothelial growth factor production and increased blood vessel extension. *Biology of Reproduction* **65** 1014–1019.

Moor RM & Seamark RF 1986 Cell signalling, permeability and microvasculatory changes during antral follicle development in mammals. *Journal of Dairy Science* **69** 927–943.

Murata T, Nakagawa K, Khalil A, Ishibashi T, Inomata H & Sueishi K 1996 The relation between expression of vascular endothelial growth factor and breakdown of the blood–retinal barrier in diabetic rat retinas. *Laboratory Investigation* **74** 819–825.

Murdoch WJN & Dunn KJ 1983 Dynamics of ovarian blood supply to periovulatory follicles of the ewe. *Biology of Reproduction* **28** 1001–1006.

Nehls V, Denzer K & Drenckhahn D 1992 Pericyte involvement in capillary sprouting during angiogenesis *in situ*. *Cell and Tissue Research* **270** 469–474.

Neufeld G, Cohen T, Gengrinovitch S & Poltorak Z 1999 Vascular endothelial growth factor (VEGF) and its receptors. *FASEB Journal* **13** 9–22.

Nicosia RF & Villaschi S 1995 Rat aortic smooth muscle cells become pericytes during angiogenesis *in vitro*. *Laboratory Investigation* **73** 658–666.

Polak JM & Van Noorden S 1997 Multiple immunostaining. In *Microscopy Handbooks no. 37: Introduction to Immunocytochemistry*, pp 73–80. Oxford: Bios Scientific Publishers.

Redmer DA & Reynolds LP 1996 Angiogenesis in the ovary. *Reviews of Reproduction* **1** 182–192.

Redmer DA, Doraiswamy V, Bortnem BJ, Fisher K, Jablonka-Shariff A, Grazul-Bilska AT & Reynolds LP 2001 Evidence for a role of capillary pericytes in vascular growth of the developing ovine corpus luteum. *Biology of Reproduction* **65** 879–889.

Reynolds LP, Grazul-Bilska AT & Redmer DA 2000 Angiogenesis in the corpus luteum. *Endocrine* **12** 1–9.

Robinson CJ & Stringer SE 2001 The splice variants of vascular endothelial growth factor (VEGF) and their receptors. *Journal of Cell Science* **114** 853–865.

Scholzen T & Gerdes J 2000 The Ki-67 protein: from the known and the unknown. *Journal of Cellular Physiology* **182** 311–322.

Shimizu T, Jiang JY, Sasada H & Sato E 2002 Changes of messenger RNA expression of angiogenic factors and related receptors during follicular development in gilts. *Biology of Reproduction* **67** 1846–1852.

Shimizu T, Jiang JY, Iijima K, Miyabayashi K, Ogawa Y, Sasada H & Sato E 2003 Induction of follicular development by direct single injection of vascular endothelial growth factor gene fragments into the ovary of miniature gilts. *Biology of Reproduction* **69** 1388–1393.

Shimoda K, Sato E, Tanaka T, Takeya T & Toyoda Y 1993 Morphological differentiation of the microvasculature during follicular development, ovulation and luteinization of mouse ovaries. *Development, Growth and Differentiation* **35** 431–437.

Stouffer RL 2004 The corpus luteum. In *The ovary*, pp 169–184. Eds PCK Leung & EY Adashi. London: Elsevier Academic Press.

Sutton ML, Gilchrist RB & Thompson JG 2003 Effects of in-vivo and in-vitro environments on the metabolism of the cumulus–oocyte complex and its influence on oocyte developmental capacity. *Human Reproduction Update* **9** 35–48.

Tamanini C & De Ambrogi M 2004 Angiogenesis in developing follicle and corpus luteum. *Reproduction in Domestic Animals* **39** 206–216.

Tilton RG, Kilo C & Williamson JR 1979 Pericyte–endothelial relationships in cardiac and skeletal muscle capillaries. *Microvascular Research* **18** 325–335.

Towbin H, Staehelin T & Gordon J 1979 Electrophoretic transfer of proteins from polyacrilamide gels to nitrocellulose sheets: procedure and some applications. *PNAS* **76** 4350–4354.

Weidner N, Semple JP, Welch WR & Folkman J 1991 Tumor angiogenesis and metastasis-correlation in invasive breast carcinoma. *New England Journal of Medicine* **324** 1–8.

Wulff C, Wiegand SJ, Saunders PT, Scobie GA & Fraser HM 2001 Angiogenesis during follicular development in the primate and its inhibition by treatment with truncated Flt-1-Fc (vascular endothelial growth factor Trap (A40)). *Endocrinology* **142** 3244–3254.

Wulff C, Wilson H, Wiegand SJ, Rudge JS & Fraser HM 2002 Prevention of thecal angiogenesis, antral follicular growth, and ovulation in the primate by treatment with vascular endothelial growth factor Trap R1R2. *Endocrinology* **143** 2797–2807.

Zimmermann RC, Hartman T, Kavic S, Pauli SA, Bohlen P, Sauer Mv & Kitajewski J 2003 Vascular endothelial growth factor receptor 2-mediated angiogenesis is essential for gonadotropin-dependent follicle development. *Journal of Clinical Investigation* **112** 659–669.

Zondek B, Sulman F & Black R 1945 The hyperemia effect of gonadotropins on the ovary. *Journal of the American Medical Association* **128** 939–944.

Received in final form 7 October 2005
Accepted 17 October 2005
Made available online as an Accepted Preprint 9 November 2005